Coded aperture detector: an image sensor with sub 20-nm pixel resolution

Ryan Miyakawa,[1,*] Rafael Mayer,[2] Antoine Wojdyla,[1] Nicolas Vannier,[2] Ian Lesser,[1] Shifrah Aron-Dine,[1] and Patrick Naulleau[1]

[1]*Lawrence Berkeley National Lab*
1 Cyclotron Rd, Berkeley, CA, 94720, USA
[2]*École Nationale Supérieure d'Ingénieurs de Caen (ENSICAEN)*
6 Boulevard Marchal Juin, 14000 Caen, France
[*]*rhmiyakawa@lbl.gov*

http://www.cxro.lbl.gov

Abstract: We describe the coded aperture detector, a novel image sensor based on uniformly redundant arrays (URAs) with customizable pixel size, resolution, and operating photon energy regime. In this sensor, a coded aperture is scanned laterally at the image plane of an optical system, and the transmitted intensity is measured by a photodiode. The image intensity is then digitally reconstructed using a simple convolution. We present results from a proof-of-principle optical prototype, demonstrating high-fidelity image sensing comparable to a CCD. A 20-nm half-pitch URA fabricated by the Center for X-ray Optics (CXRO) nano-fabrication laboratory is presented that is suitable for high-resolution image sensing at EUV and soft X-ray wavelengths.

OCIS codes: (110.1758) Computational imaging; (110.1220) Apertures.

References and links

1. C. Wagner, J. Bacelar, N. Harned, E. Loopstra, S. Hendriks, I. de Jong, P. Kuerz, L. Levasier, M. van de Kerkhof, M. Lowisch, H. Meiling, D. Ockwell, R. Peeters, E. van Setten, J. Stoeldraijer, S. Young, J. Zimmerman, and R. Kool, "EUV lithography at chipmakers has started: performance validation of ASML's NXE:3100." Proc. SPIE 7969, 79691F (April, 2011).
2. R. Hain, C. J. Kushler, and C Tropea. "Comparison of CCD, CMOS and intensified cameras." Exp. Fluids **42**(3) 403–411 (2007).
3. P. E. Murphy, J. Fleig, G. Forbes, and M. Tricard. "High precision metrology of domes and aspheric optics," Proc. SPIE 5786 (May 2005)
4. J. L. Culhane, L. K. Harra, A. M. James, K. Al-Janabi, L. J. Bradley, R. A. Chaudry, K. Rees, J. A. Tandy, P. Thomas, M. C. R. Whillock, B. Winter, G. A. Doschek, C. M. Korendyke, C. M. Brown, S. Myers, J. Mariska, J. Seely, J. Lang, B. J. Kent, B. M. Shaughnessy, P. R. Young, G. M. Simnett, C. M. Castelli, S. Mahmoud, H. Mapson-Menard, B. J. Probyn, R. J. Thomas, J. Davila, K. Dere, D. Windt, J. Shea, R. Hagood, R. Moye, H. Hara, T. Watanabe, K. Matsuzaki, T. Kosugi, V. Hansteen, . Wikstol. "The EUV imaging spectrometer for Hinode," Sol. Phys. **243**(1) 19–61 (2007).
5. D. Tichenor, A. W. Replogle, S. H. Lee, W. Ballard, A. Leung, G. Kubiak, L. Klebanoff, J. Graham, S. J. Goldsmith, M. K. Jefferson, J. Wronosky, T. Smith, T. Johnson, H. Shields, L. Hale, H. Chapman, J. Taylor, D. Sweeney, J. Folta, G. Sommargren, K. Goldberg, P. Naulleau, D. T. Attwood, E. Gullikson, "Performance upgrades in the EUV engineering test stand," Proc. SPIE 4688, (July 2002)
6. R. Accorsi, F. Gasparini, and R. C. Lanza. "A coded aperture for high-resolution nuclear medicine planar imaging with a conventional Anger camera: experimental results," IEEE Trans. Nucl. Sci. **48**(6) 2411–2417 (2001).
7. S. Eisebitt, "X-ray holography: the hole story," Nature Photon. **2** 529-530 (2008).

#212657 - $15.00 USD Received 23 May 2014; revised 25 Jun 2014; accepted 1 Jul 2014; published 8 Aug 2014

8. S. R. Gottesman and E. E. Fenimore, "New family of binary arrays for coded aperture imaging," Appl. Opt. **28**(20) 4344–4352 (1989).

1. Introduction

In certain optical experiments, spatial light intensity distributions cannot be easily measured by a conventional CCD camera. This can occur for a number of reasons. First, some experiments involve light distributions having critical dimensions that are much smaller than a CCD pixel. For example, in the case of photolithography steppers in the semiconductor industry, the critical dimensions of the relevant features can be less than 25 nm for state-of-the-art tools [1], which is nearly 200 times smaller than the pixel size of a typical CCD sensor [2]. Second, some experiments require the measurement of light distributions that have large spatial extent. Interferometers and lensless imaging systems designed at high numerical apertures can produce intensity profiles that are much larger than conventional CCD sensors can support [3]. Finally, practical considerations such as cost and design can plague systems operating in certain photon energy regimes. Extreme ultraviolet (EUV) or Soft X-ray (SXR) CCDs for instance must operate in vacuum, which can impose strict design constraints associated with cooling and outgassing. Additionally, these sensors may require back-thinning and a back-illumination configurations to reduce absorption in the substrate, which drives up the cost of the cameras [4].

The coded aperture detector is an alternative image sensor that is well-suited to accommodate these concerns. With customizable sensor size and pixel resolution, the coded aperture detector can be tailored to meet the demands of experiments involving nearly all ranges of spatial light distributions. The detector can be chosen to accommodate a wide variety of spectral regimes, and is typically much more cost-effective than a CCD.

2. Working principle

In the coded aperture detector, light intensity in the image plane is incident on a defined structure with known geometry (the so-called *coded aperture*), and the transmitted scattered energy is measured by a photodiode. The coded aperture is then raster-scanned and intensity values are collected at each scan position. This collection of measurements defines a linear system of equations which is then solved to reconstruct the intensity profile. Because the measurement relies solely on the energy transmitted by the aperture, this process is not affected by partial coherence or finite spectral bandwidth provided that the photodiode has adequate sensitivity over the spectral region in question.

The idea of creating a scanning, diode-based intensity sensor has been previously established using simple apertures [5]. One common configuration is implemented by raster-scanning a aperture of diameter d at the image plane of the optical system. Here, d defines the resolution of the measurement and is chosen to accommodate the smallest desired feature in the image. If the intensity distribution at the image plane is $a(x,y)$ and the intensity transmittance function of the aperture is $t(x,y)$, then the intensity $i(x,y)$ measured by the diode at each scan location (x,y) is given by,

$$i(x,y) = (a * t)(x,y) \tag{1}$$

where $*$ denotes convolution. While this sensor works well for many applications, it becomes less effective when higher resolution (hence smaller d) is required since the photon flux through the aperture becomes small relative to the intrinsic noise of the system.

The coded aperture detector addresses this problem by choosing $t(x,y)$ to have a higher efficiency while maintaining the resolution of the process. From Eq. (1), we can interpret the coded aperture detector as a linear system characterized by an impulse response defined by the

#212657 - $15.00 USD Received 23 May 2014; revised 25 Jun 2014; accepted 1 Jul 2014; published 8 Aug 2014

aperture transmittance function $t(x,y)$. Solving for $a(x,y)$ represents a standard deconvolution problem, and thus care must be taken in choosing the coded aperture transmittance spectrum $T(f_x,f_y)$ to have both an acceptable bandwidth to accommodate the spatial frequency distribution of the image intensity, as well as an absence of nulls that reduce the sensitivity of the measurement at certain frequencies and complicate the reconstruction in the presence of noise.

To summarize, the coded aperture transmittance function should be designed to satisfy the following criteria:

1. $t(x,y)$ should have a high throughput relative to the intrinsic noise of the system.
2. The width of the transmittance spectrum $T(f_x,f_y)$ should be large enough to accommodate all of the desired spatial frequencies of the intensity distribution spectrum $U(f_x,f_y)$.
3. The transmittance spectrum $T(f_x,f_y)$ should be relatively flat, to allow for a well-conditioned deconvolution in the presence of noise.

3. Uniformly redundant arrays (URAs)

Uniformly redundant arrays describe a class of matrices with mathematical properties that are well-suited to the transmittance function requirements enumerated above. When a URA is realized as a discrete 2-dimensional function, it has high efficiency due to its 50% duty cycle, a flat spectrum, and a customizable cutoff frequency. For these same reasons, URAs have found great success in the fields of coded aperture imaging and lensless imaging [6, 7].

In this paper, we will take URA to mean the *modified* uniformly redundant array, a subclass of URAs consisting of $N \times N$ square matrices described by Gottesman and Fenimore [8]. Among the key properties of these arrays is that for every URA $u(x,y)$, there exists a complementary function $u'(x,y)$ such that

$$(u \otimes u')(x,y) = \delta(x,y) \tag{2}$$

where $\otimes$ denotes circular convolution and $\delta(x,y)$ is the Dirac delta function. The definition of $u(x,y)$ and $u'(x,y)$ can be found in the literature. We can leverage this property by creating a so-called *tiled* URA $u_T(x,y)$, defined as:

$$u_T(x,y) = u(x \bmod N, y \bmod N) \tag{3}$$

Using this tiled URA as the scanning aperture, $t(x,y) = u_T(x,y)$, Eq. (1) gives:

$$\begin{aligned} i(x,y) &= (a * u_T)(x,y) \\ &= (a \otimes u)(x,y) \end{aligned} \tag{4}$$

The measured intensity can then be digitally post-processed by performing a circular convolution with u' to reconstruct $a(x,y)$:

$$\begin{aligned} (i \otimes u')(x,y) &= [(a \otimes u) \otimes u'](x,y) \\ &= [a \otimes (u \otimes u')](x,y) \\ &= [a \otimes \delta](x,y) \\ &= a(x,y) \end{aligned} \tag{5}$$

In the URA-based coded aperture, the field of view is set by the URA diameter, and the resolution is set by the dimension of its smallest feature. Both of these variables can be customized

#212657 - $15.00 USD Received 23 May 2014; revised 25 Jun 2014; accepted 1 Jul 2014; published 8 Aug 2014

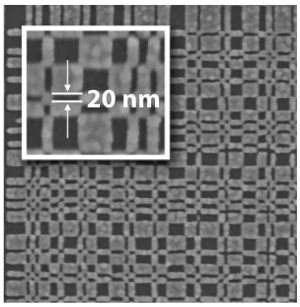

Fig. 1. SEM image of a URA fabricated at the Center for X-ray Optics demonstrating 20-nm resolution. The pattern consists of a 80-nm gold absorber on a silicon nitride membrane

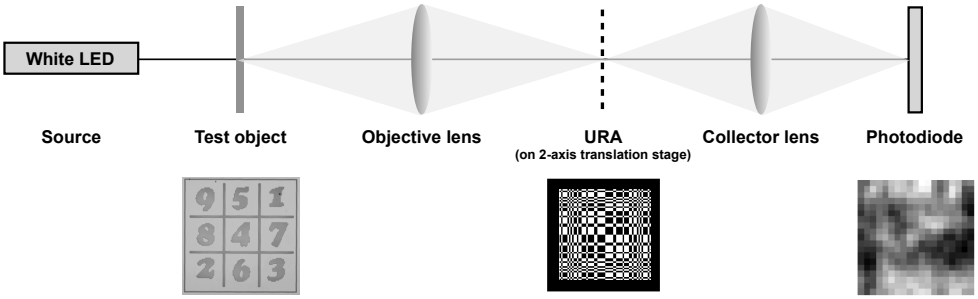

Fig. 2. Schematic of visible light prototype.

to accommodate the requirements of applications on a case-by-case basis. For example, in the case of a shearing interferometer where a larger sensor is required, a 509×509 pixel URA could be made to have 200-um pixels to create a 4-inch sensor. Alternatively, to build an EUV aerial image monitor for a lithography tool, the URA could be designed to have 20-nm pixels to resolve nanoscale intensity profiles. Recently the Center for X-ray Optics nanofabrication laboratory demonstrated a URA with 20-nm resolution, using a gold absorber on a silicon nitride membrane as shown in Fig. 1. This URA is suitable for use for ultra high-resolution image sensing in the EUV and soft x-ray regimes.

4. Experimental setup

To validate the working principle of the coded aperture detector, a visible-light prototype was set up on an optical bench using a white light LED source. A schematic of this setup is shown

#212657 - $15.00 USD Received 23 May 2014; revised 25 Jun 2014; accepted 1 Jul 2014; published 8 Aug 2014

in Fig. 2. An objective lens images a test object to the coded aperture which is mounted to a 2-axis translation stage. The aperture is raster-scanned, and the transmitted light intensity is captured by a collector lens and focused on to a photodiode. This collector lens is optional, and was used here to increase the working distance between the coded aperture stage and the diode; in other experiments, it may be desirable to place the diode directly after the coded aperture. The diode current is preprocessed by an amplifier, and the resulting signal is digitized and read into a computer where the image is reconstructed.

Test objects and URA coded apertures of various sizes were printed in chromium-on-quartz photomasks, consisting of binary patterns with 20-um square pixels. The conjugate planes were set at twice the focal length of the objective lens to provide unity magnification, eliminating a possible pixel mismatch between the image intensity and the coded aperture. The test pattern mask also included a checkerboard pattern that was used to align the relative tip, tilt, and rotation of the conjugate planes.

A MATLAB interface was used to control the position of the stages and record the diode current. The reconstruction is performed in the Fourier domain, and takes only a few milliseconds to compute on a standard desktop machine.

5. Results

We present results from two test objects, a sudoku puzzle and a Berkeley Lab logo (shown in Figs. 3(a) and 3(b)). A 179×179 pixel URA was used as the coded aperture, which was tiled into a 3×3 array. The size of this URA was chosen to be greater than the size of each of the test objects to ensure that the light at the image plane would fit within one URA tile.

Figures 3(c)–3(f) show the captured diode signal and the reconstructed image intensity demonstrating high fidelity images compared with the corresponding object profiles. Single pixels are resolved in the curved line above the "BERKELEY LAB" text in the LBL logo, demonstrating that the coded aperture detector is able to operate near its theoretical resolution limit.

To obtain a quantitative metric on the resolution of the prototype sensor, we estimate the point spread function (PSF) of the system by modeling it as a Gaussian function of the form:

$$PSF(x,y,\sigma_x,\sigma_y) = A\exp\left\{-\left(\frac{x^2}{2\sigma_x^2}-\frac{y^2}{2\sigma_y^2}\right)\right\} \tag{6}$$

Using this model, we define the merit function,

$$E(\sigma_x,\sigma_y) = \sum_{x,y}|(i_{ideal} * PSF)(x,y,\sigma_x,\sigma_y) - i_{measured}(x,y)|^2 \tag{7}$$

which is minimized against the PSF width parameters σ_x and σ_y. The results of this analysis are presented in Table 1.

Table 1. Estimation of PSF widths.

Object	PSF FWHM (x,y)	Normalized residual error
Sudoku Puzzle	(2.06 px, 2.10 px)	0.007
Berkeley Lab Logo	(1.58 px, 1.32 px)	0.003

The discrepancy between the measured PSF FWHM values and the theoretical resolution limit of 1 px can be attributed to a number of potential factors. Systematic errors include focus error, wavefront aberrations in the objective lens, and chromatic aberration. These effects are independent from the coded aperture detector and blur the intensity in the image plane. Errors

#212657 - $15.00 USD Received 23 May 2014; revised 25 Jun 2014; accepted 1 Jul 2014; published 8 Aug 2014

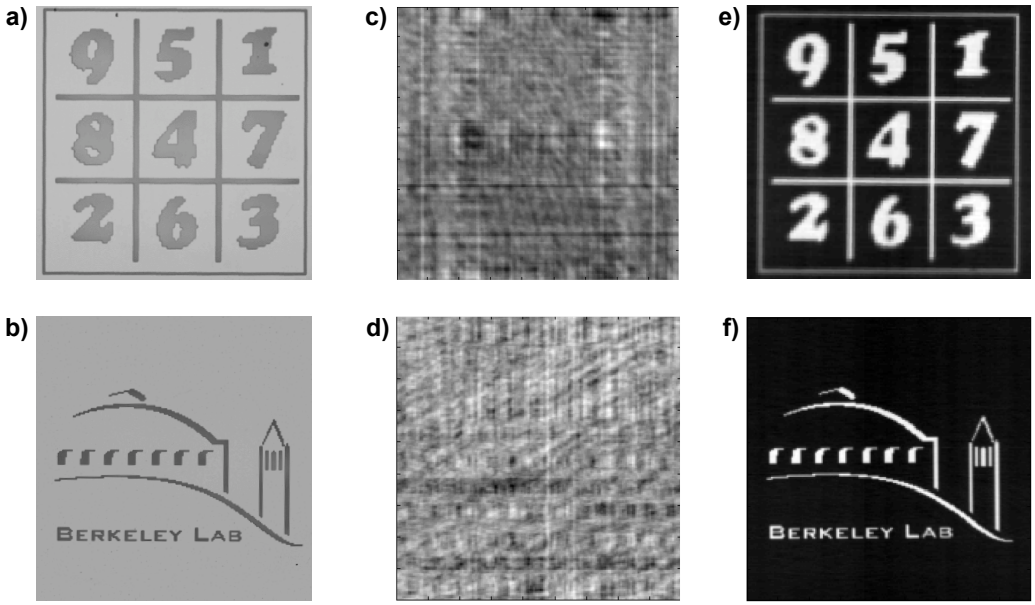

Fig. 3. (a)–(b) Pictures of the object patterns taken through an optical microscope, (c)–(d) Signal captured on the diode, and (e)–(f) Reconstructed images after processing.

directly associated with the coded aperture detector can include fabrication errors in the URA, tilt in the URA mask, and errors in the stage motion. In this experiment, we believe that a large fraction of the error was caused by defocus; the relatively short depth of focus ($\sim$ 3 um) and the lack of an automated axial translation stage made finding best-focus challenging. This hypothesis is consistent with the discrepancy in PSF widths between the sudoku puzzle and LBL logo patterns, which where measured using the same URA and similar alignment conditions.

6. Discussion

The coded aperture detector is a versatile, low-cost alternative to CCDs for applications with special image sensing requirements. An optical prototype of the detector has demonstrated high-fidelity image sensing and validated that the sensor can operate at its theoretical resolution limit. The flexibility of the of the URA-based coded aperture allows the coded aperture detector to accommodate a wide variety of experimental requirements, including small pixel size, large sensor size, and several different photon energy regimes.

The tradeoff for this versatility is the acquisition time required to scan the aperture, which prevents this sensor from providing images in real-time. This delay can make it difficult to find best-focus in applications where there is no other feedback. Additionally, the coded aperture detector requires that the relative tip, tilt, and rotation of the conjugate planes be well-characterized. Errors in these parameters cause a distortion in the effective aperture function $u(x,y)$, which can lead to artifacts in the reconstruction.

However, for many applications the coded aperture detector will open the door to image sensing that was previously unavailable. One such application is in the SEMATECH Berkeley Microfield Exposure Tool (MET), a high-resolution EUV lithography tool at LBL where the critical dimensions of features are orders of magnitude smaller than pixel sizes of commercially

#212657 - $15.00 USD Received 23 May 2014; revised 25 Jun 2014; accepted 1 Jul 2014; published 8 Aug 2014

available CCD cameras. Here, a coded aperture detector will be installed alongside the wafer to provide in-situ aerial image monitoring and aberration diagnostics.

Acknowledgments

This work was performed at LBNL's Center for X-ray Optics and was supported by SEMATECH through the U.S. Department of Energy under Contract No. DE-AC02-05CH11231.

#212657 - $15.00 USD Received 23 May 2014; revised 25 Jun 2014; accepted 1 Jul 2014; published 8 Aug 2014